



distinguish different source distributions from each other using only the measured fields. The sensing, or channel capacity of the Green's function matrix can be used to compactly assess the imaging capabilities of the compressive antenna. For high Signal to Noise Ratios (SNR), the sensing capacity can be expressed as [10]:

$$C \approx T \log_2 \left( \sum_{t=1}^T \frac{P_t}{N_0} \right) + \sum_{t=1}^T \log_2 \left( \frac{\sigma_t^2}{T} \right) \quad (3)$$

The proposed antenna design method seeks to maximize the sensing capacity of the Green's function matrix by optimizing the constitutive parameters  $\mu(\mathbf{r}, \omega)$  and  $\epsilon(\mathbf{r}, \omega)$  of the scattering elements placed upon the reflector. Since the channel capacity penalizes over the logarithm of the singular values, this approach favors systems with small condition numbers  $\sigma_{\max}/\sigma_{\min}$ .

### III. A GENERAL DESIGN APPROACH

In the optimization problem, the transmitting antenna system is described by a set of current sources located at  $T$  locations. Each transmitting antenna excites the  $M$  positions in the imaging region with stepped-frequency waveforms at  $K$  frequencies. The design procedure optimizes the constitutive properties  $\epsilon(\mathbf{r}, \omega)$  and  $\mu(\mathbf{r}, \omega)$  of scattering elements located at  $N$  positions along the reflector. In order to allow the scattering elements to be dispersive, the permittivity and permeability of the scatterers at the  $k$ -th frequency will be jointly represented by the variable  $\mathbf{x}_k$ . With this convention, the matrix  $\mathbf{G}_k(\mathbf{x}_k) \in \mathbb{C}^{3M \times 3T}$  can be defined as the Green's function matrix for sources radiating at frequency  $\omega_k$ , located at the  $T$  transmitter positions, and evaluated at the  $M$  positions in the imaging region. This matrix is a nonlinear function of the design variables  $\mathbf{x}_k$ . By concatenating the Green's function matrices for multiple frequencies, the multi-frequency Green's function matrix  $\mathbf{G}(\mathbf{x}) \in \mathbb{C}^{3M \times 3KT}$  can be expressed as:

$$\begin{aligned} \mathbf{G}(\mathbf{x}) &= \mathbf{G}(\mathbf{x}_1, \mathbf{x}_2, \dots, \mathbf{x}_K) \\ &= [\mathbf{G}_1(\mathbf{x}_1), \mathbf{G}_2(\mathbf{x}_2), \dots, \mathbf{G}_K(\mathbf{x}_K)] \end{aligned} \quad (4)$$

where the vector  $\mathbf{x}$  is the vector of concatenated design variables for each frequency. Assuming that  $M > KT$ , the channel capacity maximization problem can be expressed as a non-convex "max-det" problem:

$$\begin{aligned} &\text{maximize} \quad \log \det (\mathbf{G}^H(\mathbf{x})\mathbf{G}(\mathbf{x})) \\ &\text{subject to} \quad h_q(\mathbf{x}) \leq 0, \quad q = 1, \dots, Q \\ &\quad \quad \quad c_p(\mathbf{x}) = 0, \quad p = 1, \dots, P \end{aligned} \quad (5)$$

It is easy to show that maximizing the log-determinant of the Gramian matrix is equivalent to maximizing the channel capacity. Since  $\mathbf{G}^H(\mathbf{x})\mathbf{G}(\mathbf{x}) = \mathbf{V}(\mathbf{x})\Sigma^2(\mathbf{x})\mathbf{V}^H(\mathbf{x})$ ,  $\log \det (\mathbf{G}^H(\mathbf{x})\mathbf{G}(\mathbf{x})) = \sum_{t=1}^T \log (\sigma_t^2)$ , which differs from the channel capacity defined in Eq. 3 only by constants.

The constraint functions  $h_q(\mathbf{x})$  and  $c_p(\mathbf{x})$  can be non-convex and depend upon the specific design constraints placed on the dielectric scatterers. For example, if the scatterers are restricted to non-dispersive materials, then the equality constraint functions force the design variables  $\mathbf{x}_1, \mathbf{x}_2, \dots, \mathbf{x}_K$  to produce

the same permittivity and conductivity. As another example, if metamaterial scattering elements are disallowed, then the inequality constraint functions force the design variables to produce dielectric constants  $\geq 1$ .

### IV. A SIMPLIFIED DESIGN APPROACH

This section describes how to solve a simplified version of Eq. 5. In this approach, both the scatterers and the background medium at the scatterer locations are assumed to be non-dispersive and non-conductive, so that the design variables  $\mathbf{x}_1, \mathbf{x}_2, \dots, \mathbf{x}_K$  are equal and are real-valued. Moreover, the constraints simply restrict the electric permittivities and magnetic permeabilities of the scatterers to lie within specified ranges,  $[\epsilon_L, \epsilon_R]$  and  $[\mu_L, \mu_R]$ . The simplified optimization problem can therefore be expressed as:

$$\begin{aligned} &\text{maximize} \quad \log \det (\mathbf{G}^H(\mathbf{x})\mathbf{G}(\mathbf{x})) \\ &\text{subject to} \quad \mathbf{x}_L \leq \mathbf{x} \leq \mathbf{x}_R \end{aligned} \quad (6)$$

Eq. 6 can be solved efficiently using the nonlinear conjugate gradient method [11]. This method requires expressions for the gradient of the cost function  $\log \det \mathbf{F}(\mathbf{x}) = \log \det (\mathbf{G}^H(\mathbf{x})\mathbf{G}(\mathbf{x}))$ . Assuming that  $\mathbf{F}(\mathbf{x})$  that is invertible, the partial derivatives  $\frac{\partial}{\partial x_l} \log \det \mathbf{F}(\mathbf{x})$  and  $\frac{\partial \mathbf{F}(\mathbf{x})}{\partial x_l}$  are:

$$\frac{\partial}{\partial x_l} \log \det \mathbf{F}(\mathbf{x}) = \text{tr} \left( \mathbf{F}^{-1}(\mathbf{x}) \frac{\partial \mathbf{F}(\mathbf{x})}{\partial x_l} \right) \quad (7)$$

$$\frac{\partial \mathbf{F}(\mathbf{x})}{\partial x_l} = \left( \frac{\partial \mathbf{G}(\mathbf{x})}{\partial x_l} \right)^H \mathbf{G}(\mathbf{x}) + \mathbf{G}^H(\mathbf{x}) \frac{\partial \mathbf{G}(\mathbf{x})}{\partial x_l} \quad (8)$$

A close examination of Eq. 4 reveals that the partial derivatives  $\frac{\partial \mathbf{G}(\mathbf{x})}{\partial x_l}$  consist of the partial derivatives  $\frac{\partial \mathbf{G}_k(\mathbf{x})}{\partial x_l}$ . By defining  $\mathbf{H}_k(\mathbf{x})$  as the discretized version of the Helmholtz operator for frequency  $k$ , the Green's function matrix  $\mathbf{G}_k(\mathbf{x})$  can be expressed as:

$$\mathbf{G}_k(\mathbf{x}) = \Phi \mathbf{H}_k^{-1}(\mathbf{x}) \Psi \quad (9)$$

where  $\Phi \in \mathbb{C}^{3M \times 3L}$ ,  $\mathbf{H}_k(\mathbf{x}) \in \mathbb{C}^{3L \times 3L}$ , and  $\Psi \in \mathbb{C}^{3L \times 3T}$ . The matrices  $\Phi$  and  $\Psi$  are subsampling matrices corresponding to the imaging and transmitter positions respectively. From this relationship, the partial derivatives  $\frac{\partial \mathbf{G}_k(\mathbf{x})}{\partial x_l}$  take the following form:

$$\frac{\partial \mathbf{G}_k(\mathbf{x})}{\partial x_l} = -\Phi \mathbf{H}_k^{-1}(\mathbf{x}) \frac{\partial \mathbf{H}_k(\mathbf{x})}{\partial x_l} \mathbf{H}_k^{-1}(\mathbf{x}) \Psi \quad (10)$$

The elements of the partial derivative matrix  $\frac{\partial \mathbf{H}_k(\mathbf{x})}{\partial x_l}$  differ depending upon whether  $x_l$  is permittivity or permeability. If  $x_l$  is the permittivity  $\epsilon_j$  at position  $j$ , then the partial derivative matrix takes the form:

$$\frac{\partial \mathbf{H}_k(\mathbf{x})}{\partial \epsilon_j} = \omega_k^2 \text{diag}(\mathbf{1}_3 \otimes \delta_{ij}) \quad (11)$$

where  $\otimes$  is the Kronecker product and  $\delta_{ij} \in \mathbb{C}^L$  is the Kronecker delta function expressed as a vector, i.e. the  $j$ -th element of  $\delta_{ij}$  equals one and all others equal zero. If  $x_l$  is

the permeability  $\mu_j$  at position  $j$ , then the partial derivative matrix takes the form:

$$\frac{\partial \mathbf{H}_k(\mathbf{x})}{\partial \mu_j} = -\frac{1}{\mu_j^2} \mathbf{L}_c \text{diag}(\mathbf{1}_3 \otimes \delta_{ij}) \mathbf{L}_c \quad (12)$$

where  $\mathbf{L}_c$  is the discretized curl operator. Computation of these derivatives requires  $K(N+T)$  calls to a forward model solver at each iteration in order to compute the necessary Green's functions.

## V. RESULTS

This sections presents preliminary antenna design results, which were generated using the simplified algorithm and a 2D forward model solver based on finite differences in the frequency domain (FDFD) [12]. The design method was executed for two different antenna configurations, where the antenna operated in reflection mode and transmission mode. In reflection mode, dielectric scatterers are added to the surface of a Perfect Electric Conductor (PEC) reflector in order to further perturb the fields scattered by the reflector. In transmission mode, dielectric scatterers are placed in between the transmitting antennas and the imaging region in order to perturb the fields that otherwise radiate in the homogeneous background medium.

Figures 1a and 1b display the design configurations for the reflection and transmission mode problems respectively. In both modes, three line source antennas, represented by the white circles, were used to excite the free-space imaging region, colored in orange. The green pixels represent the locations of the scatterers to be optimized, and the red pixels in the reflection mode configuration represent the PEC. The antennas were constrained to transmit at five frequencies linearly spaced between 3.1GHz and 3.5GHz, and the dielectric constant of the scatterers was constrained to the range  $[1, 10]$ ; the magnetic permeability was restricted to  $\mu = \mu_0$ .

Figure 2a displays the optimized permittivity distribution for the reflection mode problem. It is important to note that the design problem of Eq. 6 is non-convex, and so it is probable that the solution displayed in Figure 2a is only a locally optimal solution. In practice, the optimization problem can be solved several times using different starting points until an antenna design with suitable sensing capacity is found. Figure 2b displays the  $\log_2$  of the singular values of the Green's function matrices for the original and optimized antennas. In this configuration, the optimized design increases the channel capacity by 29 bits per pixel and decreases the condition number by a factor of 22, from approximately 1510 to 69. Figures 3a and 3b display the Green's function of the middle antenna radiating at 3.5GHz for the original and optimized antennas respectively. While the phase front of the original antenna is fairly uniform as a function of distance from the transmitter, the phase front of the optimized antenna is noticeably perturbed.

Figure 4a displays the optimized permittivity distribution for the transmission mode problem, and Figure 4b displays the  $\log_2$  of the singular values of the Green's function matrices for the original and optimized antennas. In this configuration, the optimized design increases the channel capacity by 40

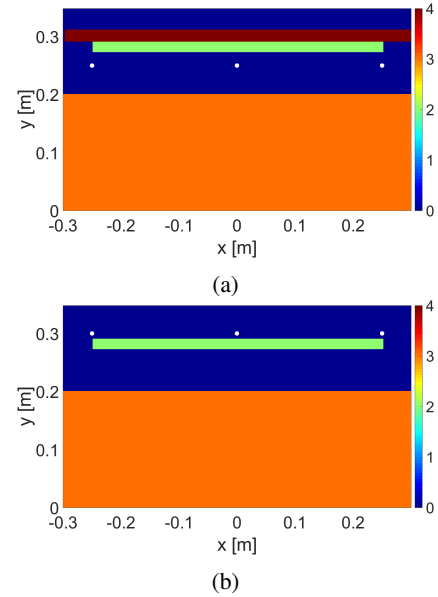


Fig. 1: Configuration for the compressive antenna operating in (a) reflector mode and (b) transmission mode. Light Blue = Transmitter locations, Orange - Imaging region, Green = Scatterer locations, Red = PEC.

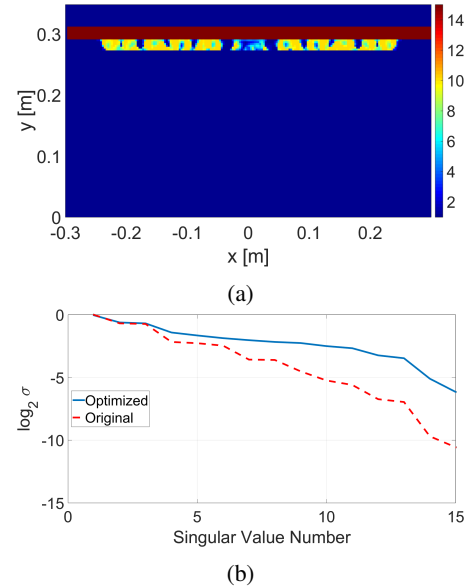


Fig. 2: Reflection mode configuration: (a) optimized permittivity. (b)  $\log_2$  of the singular values of Green's function matrices.

bits per pixel and decreases the condition number by a factor of 60, from approximately 1400 to 23. Figures 5a and 5b display the Green's function of the middle antenna radiating at 3.5GHz for the original and optimized antennas respectively. Without the PEC reflector or any scattering dielectrics, the transmitting antenna radiates isotropically, and so the phase-front is constant as a function of distance from the antenna. In comparison, the phase-front of the optimized design exhibits a pseudo-random pattern, which conveys an increased amount of information compared to the isotropic phase front.

## VI. CONCLUSIONS

This paper describes a novel, model-based antenna design method for high-sensing-capacity imaging applications. By optimizing the channel capacity of the dyadic Green's function matrix, the new approach generates antenna configurations with improved sensing and imaging capabilities. Preliminary design results using a 2D FDFD forward model for two antenna configurations, operating in transmission mode and reflection mode, demonstrate how the novel approach generates antenna configurations with improved channel capacity.

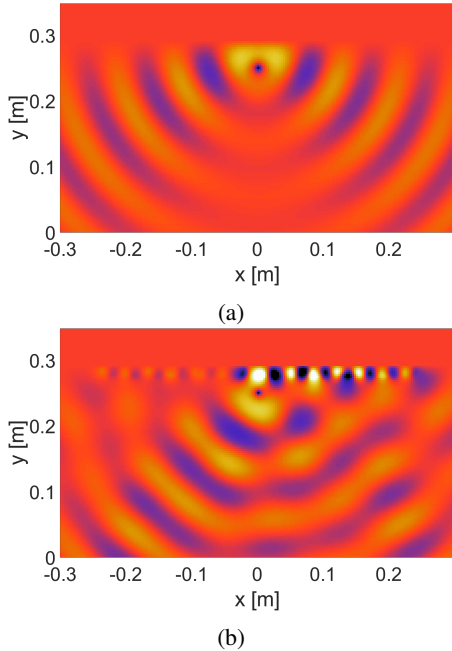


Fig. 3: Green's functions of the compressive antenna operating in reflection mode at 3.5GHz with (a) the original design and (b) optimized design.

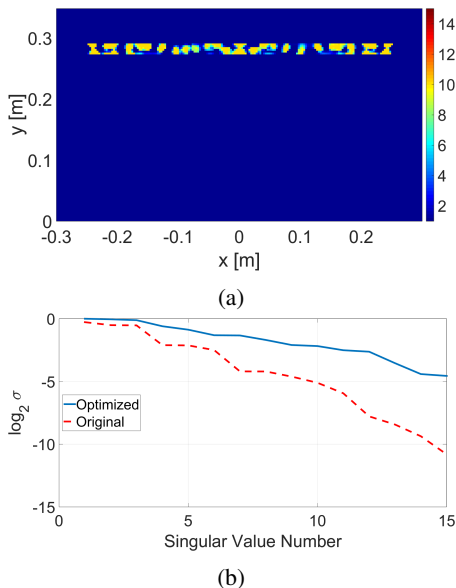


Fig. 4: Transmission mode configuration: (a) optimized permittivity. (b)  $\log_2$  of the singular values of Green's function matrices.

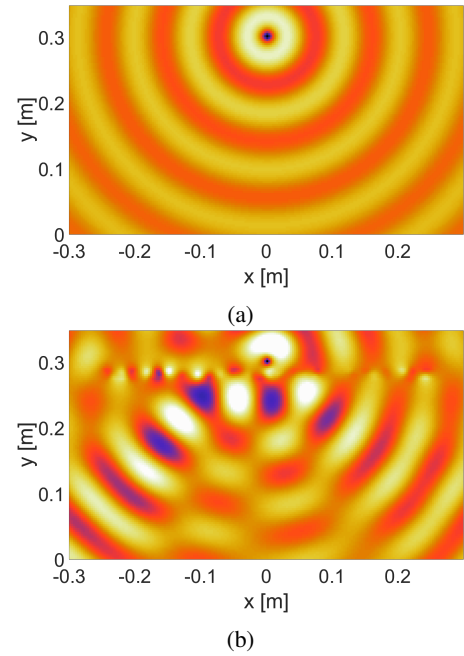


Fig. 5: Green's functions of the compressive antenna operating in transmission mode at 3.5GHz with (a) the original design and (b) optimized design.

Although this paper focused on the simplified design approach, the theory of the general design approach allows it to be applied to realistic scenarios.

## REFERENCES

- [1] J. H.-H. J. A. Martinez-Lorenzo and W. Blackwell, "A single-transceiver compressive reflector antenna for high-sensing-capacity imaging," *IEEE Antennas and Wireless Propagation Letters*, 2015.
- [2] A. M. L. T. W. B. J. Heredia-Juevas, G. Allan and J. A. Martinez-Lorenzo, "Consensus-based imaging using admm for a compressive reflector antenna," in *IEEE AP-S International Symposium*, 2015.
- [3] A. Busboom, H. D. Schotten, and H. Elders-Boll, "Coded aperture imaging with multiple measurements," *JOSA A*, vol. 14, no. 5, pp. 1058–1065, 1997.
- [4] G. D. De Villiers, N. T. Gordon, D. A. Payne, I. K. Proudler, I. D. Skidmore, K. D. Ridley, C. R. Bennett, R. A. Wilson, and C. W. Slinger, "Sub-pixel super-resolution by decoding frames from a reconfigurable coded-aperture camera: theory and experimental verification," in *SPIE Optical Engineering+ Applications*. International Society for Optics and Photonics, 2009, pp. 746 806–746 806.
- [5] R. F. Marcia and R. M. Willett, "Compressive coded aperture super-resolution image reconstruction," in *Acoustics, Speech and Signal Processing, 2008. ICASSP 2008. IEEE International Conference on*. IEEE, 2008, pp. 833–836.
- [6] E. J. Candès, J. Romberg, and T. Tao, "Robust uncertainty principles: Exact signal reconstruction from highly incomplete frequency information," *Information Theory, IEEE Transactions on*, vol. 52, no. 2, pp. 489–509, 2006.
- [7] D. L. Donoho, "Compressed sensing," *Information Theory, IEEE Transactions on*, vol. 52, no. 4, pp. 1289–1306, 2006.
- [8] A. Massa, P. Rocca, and G. Oliveri, "Compressive sensing in electromagnetics-a review," *Antennas and Propagation Magazine, IEEE*, vol. 57, no. 1, pp. 224–238, 2015.
- [9] P. Van Den Berg and A. Abubakar, "Contrast source inversion method: state of art," *Journal of Electromagnetic Waves and Applications*, vol. 15, no. 11, pp. 1503–1505, 2001.
- [10] J. G. Proakis and M. Salehi, *Digital communications*, 5, Ed. McGraw-Hill, 2008.
- [11] J. Nocedal and S. J. Wright, "Numerical optimization 2nd," 2006.

- [12] C. Rappaport, A. Morgenthaler, and M. Kilmer, "FDFD modeling of plane wave interactions with buried objects under rough surfaces,," in *2001 IEEE Antenna and Propagation Society International Symposium*, 2001, p. 318.